Nuclear Instruments and Methods in Physics Research A 742 (2014) 158–161

Contents lists available at ScienceDirect

Nuclear Instruments and Methods in Physics Research A

journal homepage: www.elsevier.com/locate/nima

Analysis on H spectral shape during the early 2012 SEPs with the PAMELA experiment

M. Martucci [n,q,*], M. Boezio [h], U. Bravar [u], R. Carbone [h], E.R. Christian [w], G.A. De Nolfo [w], M. Mergè [k,n], E. Mocchiutti [h], R. Munini [h,o], M. Ricci [q], J.M. Ryan [u], A. Sotgiu [n], S. Stochaj [v], N. Thakur [w], O. Adriani [a,b], G.C. Barbarino [c,d], G.A. Bazilevskaya [e], R. Bellotti [f,g], E.A. Bogomolov [i], M. Bongi [a,b], V. Bonvicini [h], S. Bottai [b], A. Bruno [g], F. Cafagna [g], D. Campana [d], P. Carlson [j], M. Casolino [k,l], G. Castellini [m], C. De Donato [k], M.P. De Pascale [k,n,1], C. De Santis [k,n], N. De Simone [k], V. Di Felice [k], V. Formato [h,o], A.M. Galper [p], A.V. Karelin [p], S.V. Koldashov [p], S. Koldobskiy [p], Y. Krutkov [i], A.N. Kvashnin [e], A. Leonov [p], V. Malakhov [p], L. Marcelli [n], A.G. Mayorov [p], W. Menn [r], V.V. Mikhailov [p], A. Monaco [g], N. Mori [b], G. Osteria [d], F. Palma [k,n], P. Papini [b], M. Pearce [j], P. Picozza [k,n], C. Pizzolotto [s,t,2], S.B. Ricciarini [b], R. Sarkar [h], V. Scotti [c,d], M. Simon [r], R. Sparvoli [k,n], P. Spillantini [a,b], Y.I. Stozhkov [e], A. Vacchi [h], E. Vannuccini [b], G. Vasilyev [i], S.A. Voronov [p], Y.T. Yurkin [p], G. Zampa [h], N. Zampa [h], V.G. Zverev [p]

[a] *University of Florence, Department of Physics, I-50019 Sesto Fiorentino, Florence, Italy*
[b] *INFN, Sezione di Florence, I-50019 Sesto Fiorentino, Florence, Italy*
[c] *University of Naples "Federico II", Department of Physics, I-80126 Naples, Italy*
[d] *INFN, Sezione di Naples, I-80126 Naples, Italy*
[e] *Lebedev Physical Institute, RU-119991 Moscow, Russia*
[f] *University of Bari, Department of Physics, I-70126 Bari, Italy*
[g] *INFN, Sezione di Bari, I-70126 Bari, Italy*
[h] *INFN, Sezione di Trieste, I-34149 Trieste, Italy*
[i] *Ioffe Physical Technical Institute, RU-194021 St. Petersburg, Russia*
[j] *KTH, Department of Physics and the Oskar Klein Centre for Cosmoparticle Physics, AlbaNova University Centre, SE-10691 Stockholm, Sweden*
[k] *INFN, Sezione di Rome "Tor Vergata", I-00133 Rome, Italy*
[l] *RIKEN, Advanced Science Institute, Wako-Shi, Saitama, Japan*
[m] *IFAC, I-50019 Sesto Fiorentino, Florence, Italy*
[n] *University of Rome "Tor Vergata", Department of Physics, I-00133 Rome, Italy*
[o] *University of Trieste, Department of Physics, I-34147 Trieste, Italy*
[p] *NRNU MEPhI, RU-115409 Moscow, Russia*
[q] *INFN, Laboratori Nazionali di Frascati, Via Enrico Fermi 40, I-00044 Frascati, Italy*
[r] *Universitat Siegen, Department of Physics, D-57068 Siegen, Germany*
[s] *INFN, Sezione di Perugia, I-06123 Perugia, Italy*
[t] *Agenzia Spaziale Italiana (ASI) Science Data Center, I-00044 Frascati, Italy*
[u] *Space Science Center, University of New Hampshire, United States*
[v] *Electrical and Computer Engineering, New Mexico State University, United States*
[w] *Heliospheric Physics Laboratory, NASA/Goddard Space Flight Center, United States*

ARTICLE INFO

Available online 1 December 2013

Keywords:
PAMELA
SEPs
Protons

ABSTRACT

The satellite-borne PAMELA experiment has been continuously collecting data since 2006. This apparatus is designed to study charged particles in the cosmic radiation. The combination of a permanent magnet, a silicon strip tracker and a silicon-tungsten imaging calorimeter, and the redundancy of instrumentation allow very precise studies on the physics of cosmic rays in a wide energy range and with high statistics. This makes PAMELA a very suitable instrument for Solar Energetic Particle (SEP) observations. Not only does it span the energy range between the ground-based neutron monitor data and the observations of

* Corresponding author. Tel.: +39 0672594791.
E-mail address: matteo.martucci@roma2.infn.it (M. Martucci).

[1] Deceased.
[2] Previously at INFN, Sezione di Trieste, I-34149 Trieste, Italy.

http://dx.doi.org/10.1016/j.nima.2013.11.078

SEPs from space, but PAMELA also carries out the first direct measurements of the composition for the highest energy SEP events, including those causing Ground Level Enhancements (GLEs). In particular, PAMELA has registered many SEP events during solar cycle 24, offering unique opportunities to address the question of high-energy SEP origin. A preliminary analysis on proton spectra behaviour during this event is presented in this work.

1. Introduction

The PAMELA spectrometer [1] is a space instrument designed for the study of primary charged particles and antiparticles in a wide energy interval, mainly from tens of MeV to about 1.2 TeV (for protons). Among the many scientific goals of PAMELA there is the study of solar activity and of solar energetic particles (SEPs) [2,3].

This work shows a brief study on the averaged flux of protons of solar origin during four major events that took place in the first months of 2012 (from January to May). The issue that concerns mechanisms and sites of SEPs acceleration remains mostly unknown. Some SEPs may be produced after powerful explosive events on the Sun, which are accompanied by solar flares, coronal mass ejections (CMEs), bursts of X/γ-rays, and radio emission [4]. We know that not only a single mechanism is involved in SEP generation: the main possibilities are stochastic acceleration, shock acceleration, and acceleration by the DC electric fields in the process of magnetic reconnection. The acceleration of SEPs may take place in the flare region, solar corona, and even in the interplanetary space [5]. The energy spectrum of SEPs provides valuable information for the study of solar and interplanetary plasma processes. PAMELA provides some of the first measurements of SEPs over several orders of magnitude in energy. Thus PAMELA presents a unique opportunity to study the highest energy SEP events, bridging the gap in current SEP measurements by ACE, STEREO, and GOES, and ground-based neutron/muon monitors [6]. The 24th solar cycle began on 2008, but there was minimal activity until the early months of 2010. The first period of 2012 was rich of events [7], some of them very energetic, that were registered by PAMELA.

2. SEP events in 2012

In this work we focused on four specific events. On January 23, 2012 at 03:59 UTC, sunspot 1402 (N28W36) erupted a long-duration M8.7-class flare, followed by a very fast moving CME. According to NOAA, the subsequent flare's radiation storm was the strongest since May 2005. On January 27, at 18:37 UTC, the same sunspot region 1402 (N27W71) released a X1.7-class flare. This sunspot was rotating onto the far side of the Sun, so the starting site was not facing Earth. The explosion also produced a huge CME, but it was not Earth-oriented. On March 7, after releasing 9M-class flares in a single day, the active region 1429 (N18E31) unleashed a powerful X5.4-class flare at 00:24 UTC. It was a very long-lasting event (over 3 days) but it was not well magnetically connected with Earth. The related CME impacted the Earth on March 8. This event marked the second strongest solar flare of Cycle 24 in terms of X-ray flux. On May 17, at 01:25 UTC, a M5.1-class flare erupted from sunspot 1476 (N07W88) and caused a GLE measured by several Neutron Monitors on Earth. It is considered that the weakest flare known to have generated a GLE event. It was an impulsive event (it lasted less than a few hours), but it was very well connected with Earth. PAMELA was able to detect all these events, measuring protons spectra in the energy range from 0.08 GeV/n to about 1 GeV/n.

3. The PAMELA detector

PAMELA is a space-borne experiment designed to perform high-precision spectral measurement of charged particles of galactic, heliospheric and trapped origin over a wide energy range [1,8]. It was mounted on the Resurs-DK1 Russian satellite launched in 2006 on an elliptical and semi-polar orbit (now semi-circular), with an altitude varying between 350 km and 600 km, which is now stable at about 570 km and at an inclination of about 70°. At high latitudes, the low geomagnetic cutoff allows low-rigidity particles (down to 50 MV) to be detected and studied. The apparatus comprises a number of very high performance detectors, capable of identifying particles through the determination of charge (Z), rigidity ($R=pc/|Z|e$, p being the momentum of a particle of charge Ze) and velocity ($\beta=v/c$) over a wide energy range. The device, which is showed in Fig. 1, is built around a permanent magnet with a six-plane double-sided silicon micro-strip tracker, providing absolute charge information and track-deflection ($\eta=\pm 1/R$, with the sign depending on the sign of the charge derived from the curvature direction) information. A scintillator system, composed of three double layers of scintillators (S1, S2, S3), provides the trigger, a time-of-flight measurement and an additional estimation of absolute charge. There is a system of anticoincidences around the area between S1 and S2 (CARD), around the top part of the magnetic cavity (CAT) and around the whole magnet (CAS).

In the bottom part of the apparatus there is a silicon–tungsten imaging calorimeter, used to measure the energy released by

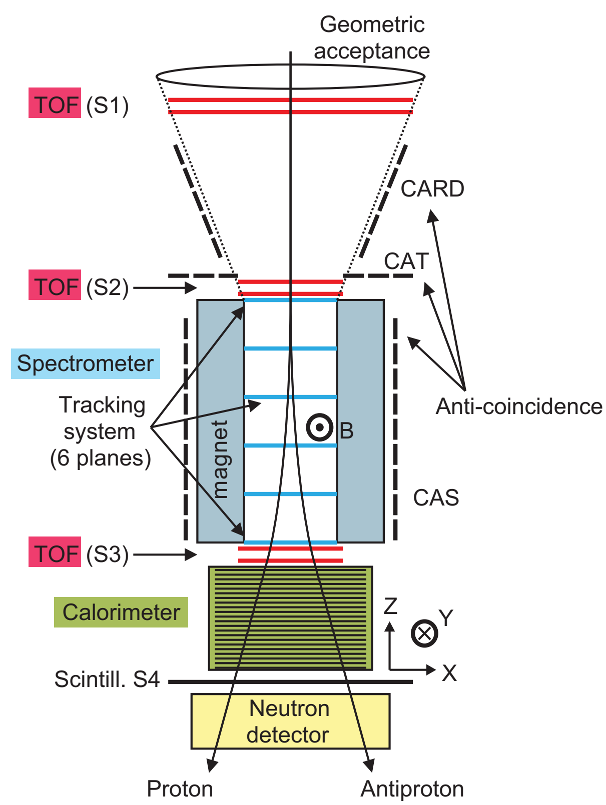

Fig. 1. Scheme of the PAMELA instrument.

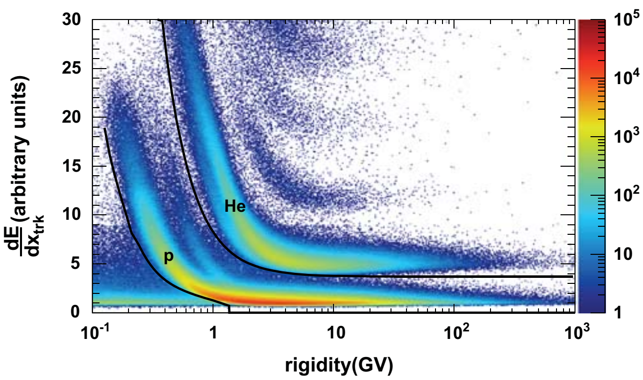

Fig. 2. Energy loss (dE/dx) vs rigidity in the PAMELA tracker. The sample of protons (p) is clearly separated from helium (He) one by rigidity-dependent cuts (solid black lines).

interacting e^+ and e^- and to reconstruct the spatial development of showers: in this way it is possible to distinguish between electromagnetic showers, hadronic showers and particles passing straight through the detector. The shower tail catcher scintillator (S4) improves the PAMELA electron–hadron separation performance by measuring shower leakage from the calorimeter. The neutron detector complements electron–proton discrimination capabilities of the calorimeter by measuring the neutron overproduction that is present in case of hadronic showers.

4. Particle selection

To obtain a clear identification of the proton sample [5] we exploit the different average energy loss of differently charged particles during their passage through matter following the *Bethe–Bloch* formula. Thus the measurement of the average energy released in the tracker for a given event at a fixed rigidity can be used to identify different particles in transit. Fig. 2 shows particle populations up to $Z \simeq 5$, and the selection bands corresponding to proton sample, that also include hydrogen isotopes. A very precise track in the spectrometer was required to reconstruct the trajectory with a fitting procedure whose goodness depends on the number of points used. Moreover, particles interacting in the satellite can produce showers of secondaries hitting the scintillator pads and producing coincidences: they are rejected with the help of anticoincidence and TOF cuts. In particular, for protons we require the absence of hits in CARD and CAT. In order to separate the primary component from the reentrant albedo one we evaluated the local geomagnetic cutoff in the Stormer approximation [9]. The value of $G = 14.9/L^2$, valid for vertically incident particles, was estimated using the IGRF magnetic field model [10]. Particles satisfying the constraint $R > 1.3\times$ cutoff were selected to remove any effect due to directionality. Albedo particles, crossing the detector from bottom to top are discarded by requiring a positive β, using the timing information of the TOF scintillators.

5. Estimation of fluxes

The absolute particle flux was obtained by dividing the measured energy spectrum by the acquisition time, the geometrical acceptance and the selection efficiencies [5]. The live time of the apparatus was provided by an on-board clock that timed the periods during which the apparatus was waiting for a trigger. The geometrical acceptance of PAMELA has been estimated by defining a fiducial area which consists of a square frame of 0.15 cm from the internal walls of the magnetic cavity, in order to ensure that all the accepted particles cross the silicon planes in the tracker without hitting the magnet walls. The corresponding geometrical factor has been estimated to be 19.93 cm^2 sr s. The efficiency of each detector selection was estimated with both flight and simulated data. The tracker efficiency has been measured selecting a sample of events that leave straight tracks in the calorimeter and do not interact hadronically. These tracks were propagated back through PAMELA acceptance, and tracker efficiency has been evaluated. A simulation was used to determine the rigidity dependence of the tracking efficiency, since this was difficult to evaluate from flight data. These results have then been compared to those obtained from flight. The total selection efficiencies have been obtained as products of tracker, dE/dx and TOF efficiencies. Finally, part of the protons may be lost due to scattering or hadronic interactions in the container in which PAMELA is housed, or in the top of the detector. Correcting for this losses is crucial for low energy analysis, so corrective factors of $\simeq 6\%$ for protons have been used [11].

6. Energy spectrum fitting

In this work we studied the proton spectral shape observed during the four major events of the first months of 2012 to obtain information on acceleration processes. We focused on a single acceleration mechanism, the first order Fermi acceleration [12]. The resulting energy spectrum of particles undergoing this mechanism turns out to be a power law with index γ, called *spectral index*.

During the propagation in the interplanetary medium, a wide variety of effects may truncate this power law-like shape of the energy spectrum. For example an adiabatic deceleration in an expanding blast wave [13], shock time scale being comparable with the time scale of particles acceleration [14] or shock spatial size being comparable with the typical dimension of particle diffusion size [15]. All these effects generate a turnover at a different energy range. From the observation of acceleration at Earth's bow shock region [16] and from interplanetary shocks [17] we could infer the form of this turnover to be exponential. So

$$\Phi_p = AE^{-\gamma}e^{-E/E_0} \tag{1}$$

where Φ_p is the proton flux intensity, A is an amplitude, E is the kinetic energy (expressed in GeV/n) and E_0 is the energy of the turnover (in GeV/n). For the present analysis we do not consider the possible effects due to Coulomb collisions or ionization losses: this means we assume that the particle density to be sufficiently low in the acceleration site to avoid these kinds of losses. The aim of this preliminary work is to catalog these four events by extracting the value of γ and E_0. We subtracted from the averaged flux the "quiet" flux measured before each flare onset: the result is a pure solar flux, which is only the result of particle injection during the event. The proton fluxes, during these events, are showed in Fig. 3. Eq. (1) has been used to fit the observed spectral shapes for both particle species, leaving the three parameters A, E_0 and γ free. These parameters, together with χ^2/NDF of the fit, are reported in Fig. 3 (a), (b), (c), (d) and summarized in Table 1. January 23 event shows a high value of γ because it was powerful and well connected. January 27 and March 7 shows a comparable steepness, infact they were both X-class flares but not well connected with Earth (so their γ is lower than the first event) . May 17 was well connected but was impulsive and weak, so its γ is the lowest. Values of E_0 appear to be of the same order of magnitude for the four events.

From Table 1 it appears evident that Eq. (1) provides a good fit for the proton spectra in all four events.

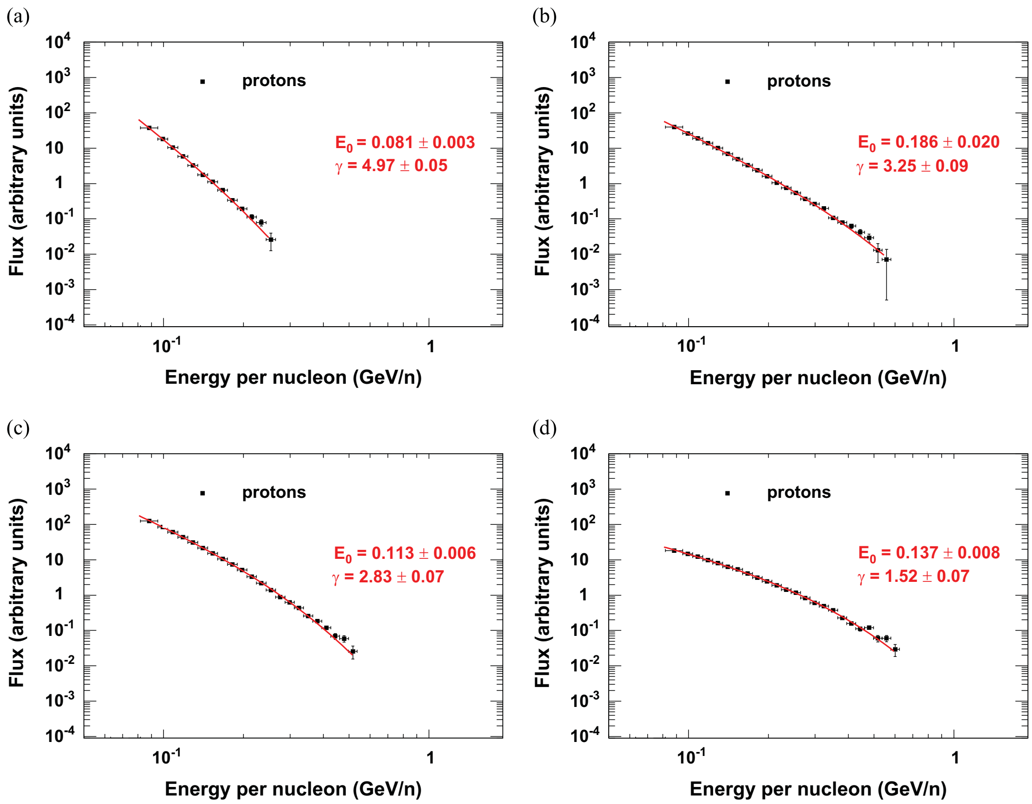

Fig. 3. Preliminary spectral fit for protons (black squares) during the events of January 23 (a), January 27 (b), March 7 (c) and May 17 (d). The red curves represent the fit with Eq. (1). (For interpretation of the references to color in this figure caption, the reader is referred to the web version of this article.)

Table 1
Preliminary data on fit parameters with Eq. (1).

Event	Class	A	E_0	γ	χ^2/NDF
Jan 23	M8.7	0.0006	0.081 ± 0.003	4.97 ± 0.05	1.88
Jan 27	X1.7	0.02	0.18 ± 0.02	3.25 ± 0.09	1.85
Mar 7	X5.4	0.3	0.11 ± 0.01	2.83 ± 0.07	1.58
May 17	M5.1	0.8	0.14 ± 0.01	1.52 ± 0.07	1.64

7. Conclusions

In this preliminary analysis we studied for the first time the shape of the solar proton flux after four SEPs events in 2012. We find that linear, first order Fermi acceleration can adequately model the first major SEPs of 2012. For each event examined, an exponential energy cutoff E_0, characterizing a finite shock size, provides a reasonable fit to the proton spectra. The values of γ seem to relate to the shock strength (higher values for powerful and Earth-directed events), while the same break energy (E_0) suggests a common development in all the events.

References

[1] P. Picozza, et al., Astroparticle Physics 27 (2007) 296.
[2] M. Casolino, et al., Advances in Space Research 37 (2006) 1848.
[3] N. De Simone, et al., in: Proceedings of 31th ICRC, Lodz, Poland, 2009.
[4] D.V. Reames, Space Science Reviews 90 (1999) 413.
[5] O. Adriani, et al., Astrophysical Journal 742 (2011) 102.
[6] M. Ricci, et al., in: Proceedings of 33rd ICRC, Rio de Janeiro, Brasil, 2013.
[7] NOAA/Space Weather Prediction Center, 〈http://www.swpc.noaa.gov/〉.
[8] N. de Simone, et al., Astrophysics and Space Sciences Transactions 7 (2011) 425.
[9] M.A. Shea, et al., Physics of the Earth and Planetary Interiors 48 (1987) 200.
[10] 〈http://www.ngdc.noaa.gov/IAGA/vmod/igrf.html〉.
[11] N. Nikonov, Ph.D. Thesis, University of Rome Tor Vergata, Italy, 2011.
[12] A.R. Bell, Monthly Notices of the Royal Astronomical Society 182 (1978) 147.
[13] M.A. Lee, et al., Space Science Reviews 33 (1982) 205.
[14] M.A. Forman, Advances in Space Research 1 (1981) 41.
[15] D.C. Ellison, Journal of Geophysical Research 90 (1984) 29.
[16] F.M. Ipavich, et al., Journal of Geophysical Research 89 (1984) 1501.
[17] D.C. Ellison, et al., Astrophysical Journal 286 (1984) 691.